

# UC Riverside

## UC Riverside Previously Published Works

### Title

A Video Bioinformatics Method to Quantify Cell Spreading and Its Application to Cells Treated with Rho-Associated Protein Kinase and Blebbistatin

### Permalink

<https://escholarship.org/uc/item/7w81t8zj>

### ISBN

978-3-319-23723-7

### Authors

Weng, Nikki Jo-Hao  
Phandthong, Rattapol  
Talbot, Prue

### Publication Date


2015

### DOI

10.1007/978-3-319-23724-4\_8

Peer reviewed

# Metadata of the chapter that will be visualized in SpringerLink

Book Title	Video Bioinformatics	
Series Title		
Chapter Title	A Video Bioinformatics Method to Quantify Cell Spreading and Its Application to Cells Treated with Rho-Associated Protein Kinase and Blebbistatin	
Copyright Year	2015	
Copyright HolderName	Springer International Publishing Switzerland	
Corresponding Author	Family Name	<b>Weng</b>
	Particle	
	Given Name	<b>Nikki Jo-Hao</b>
	Prefix	
	Suffix	
	Division	Department of Cell Biology & Neuroscience
	Organization	University of California
	Address	2320 Spieth Hall, 900 University Ave., Riverside, CA, 92507, USA
	Email	jweng002@ucr.edu
Author	Family Name	<b>Phandthong</b>
	Particle	
	Given Name	<b>Georg</b> 
	Prefix	
	Suffix	
	Division	Department Cell, Molecular, and Developmental Biology
	Organization	University of California
	Address	2320 Spieth Hall, 900 University Ave., Riverside, CA, 92507, USA
	Email	rphan005@ucr.edu
Author	Family Name	<b>Talbot</b>
	Particle	
	Given Name	<b>Prue</b>
	Prefix	
	Suffix	
	Division	Department of Cell Biology & Neuroscience
	Organization	University of California
	Address	2320 Spieth Hall, 900 University Ave., Riverside, CA, 92507, USA
	Email	talbot@ucr.edu

**Abstract** Commercial software is available for performing video bioinformatics analysis on cultured cells. Such software is convenient and can often be used to create suitable protocols for quantitative analysis of video data with relatively little background in image processing. This chapter demonstrates that CL-Quant software, a commercial program produced by DRVision, can be used to automatically analyze cell spreading in time-lapse videos of human embryonic stem cells (hESC). Two cell spreading protocols were developed and tested. One was professionally created by engineers at DRVision and adapted to this project. The other was created by an undergraduate student with 1 month of experience using CL-Quant. Both protocols successfully segmented small spreading colonies of hESC, and, in general, were in good agreement with the ground truth which was measured using ImageJ. Overall the professional protocol

performed better segmentation, while the user-generated protocol demonstrated that someone who had relatively little background with CL-Quant can successfully create protocols. The protocols were applied to hESC that had been treated with ROCK inhibitors or blebbistatin, which tend to cause rapid attachment and spreading of hESC colonies. All treatments enabled hESC to attach rapidly. Cells treated with the ROCK inhibitors or blebbistatin spread more than controls and often looked stressed. The use of the spreading analysis protocol can provide a very rapid method to evaluate the cytotoxicity of chemical treatment and reveal effects on the cytoskeleton of the cell. While hESC are presented in this chapter, other cell types could also be used in conjunction with the spreading protocol.

---



# Chapter 8

## A Video Bioinformatics Method to Quantify Cell Spreading and Its Application to Cells Treated with Rho-Associated Protein Kinase and Blebbistatin

Nikki Jo-Hao Weng, George Phandthong and Prue Talbot

**Abstract** Commercial software is available for performing video bioinformatics analysis on cultured cells. Such software is convenient and can often be used to create suitable protocols for quantitative analysis of video data with relatively little background in image processing. This chapter demonstrates that CL-Quant software, a commercial program produced by DRVision, can be used to automatically analyze cell spreading in time-lapse videos of human embryonic stem cells (hESC). Two cell spreading protocols were developed and tested. One was professionally created by engineers at DRVision and adapted to this project. The other was created by an undergraduate student with 1 month of experience using CL-Quant. Both protocols successfully segmented small spreading colonies of hESC, and, in general, were in good agreement with the ground truth which was measured using ImageJ. Overall the professional protocol performed better segmentation, while the user-generated protocol demonstrated that someone who had relatively little background with CL-Quant can successfully create protocols. The protocols were applied to hESC that had been treated with ROCK inhibitors or blebbistatin, which tend to cause rapid attachment and spreading of hESC colonies. All treatments enabled hESC to attach rapidly. Cells treated with the ROCK inhibitors or blebbistatin spread more than controls and often looked stressed. The use of the spreading analysis protocol can provide a very rapid method to evaluate the

---

N.J.-H. Weng (✉) · P. Talbot  
Department of Cell Biology & Neuroscience, University of California,  
2320 Spieth Hall, 900 University Ave., Riverside, CA 92507, USA  
e-mail: jweng002@ucr.edu

P. Talbot  
e-mail: talbot@ucr.edu

G. Phandthong  
Department Cell, Molecular, and Developmental Biology, University of California,  
2320 Spieth Hall, 900 University Ave., Riverside, CA 92507, USA  
e-mail: rphan005@ucr.edu



27 cytotoxicity of chemical treatment and reveal effects on the cytoskeleton of the cell.  
28 While hESC are presented in this chapter, other cell types could also be used in  
29 conjunction with the spreading protocol.  
30

## 31 8.1 Introduction

32 Live cell imaging has been widely used in our laboratory for many years to study  
33 dynamic cell processes [9, 18, 20, 40–42] and has more recently been applied to  
34 toxicological problems [10, 12, 22, 23, 27, 32–36, 39]. Analysis of dynamic events,  
35 such as cell attachment, migration, division, and apoptosis, can provide mechanistic  
36 insight into normal cellular processes [28, 37] as well as how toxicants affect cells  
37 [2, 5, 23, 42]. Collection of video data has recently improved due to the intro-  
38 duction of commercial incubators with built-in microscopes and cameras for col-  
39 lecting time-lapse data during short- and long-term experiments [8, 30, 37].

40 After videos are collected, it is important to extract quantitative data from them.  
41 A challenging but important issue until recently has been how to analyze large  
42 complex data sets that are produced during live cell imaging. When video data  
43 analyses are done manually by humans, many hours of personnel time are usually  
44 required to complete a project, and manual analysis by humans is subject to vari-  
45 ation in interpretation and error. Video bioinformatics software can be used to speed  
46 the analysis of large data sets collected during video imaging of cells and can also  
47 improve the accuracy and repeatability of analyses [37]. Video bioinformatics,  
48 which involves the use of computer software to mine specific data from video  
49 images, is concerned with the automated processing, analysis, understanding,  
50 visualization, and knowledge extracted from microscopic videos. Several free video  
51 bioinformatics software packages are available online such as ImageJ and  
52 Gradientech Tracking Tool ([http://gradientech.se/products/gradientech-tracking-  
53 tool/](http://gradientech.se/products/gradientech-tracking-tool/)). Also, some advanced video bioinformatics software packages, such as  
54 CL-Quant, Amira, and Cell IQ, are now commercially available and can be used to  
55 generate customized protocols or libraries to analyze video data and determine  
56 quantitatively how cells behave during experimental conditions.

57 This chapter presents a new application of CL-Quant software to automatically  
58 analyze cell spreading in time-lapse videos of human embryonic stem cells (hESC)  
59 (WiCell, Madison, WI). While hESC are presented in this chapter, other cell types  
60 could also be used in conjunction with these protocols.



## 8.2 Instrumentation Used to Collect Live Cell Video Data

### 8.2.1 BioStation IM

Data were collected with a BioStation IM. The BioStation IM or its newer version the IM-Q, manufactured by Nikon, is a bench top instrument that houses a motorized inverted microscope, an incubator with a built-in high sensitivity cooled CCD camera, and software for controlling exposures, objectives, and the type of imaging (e.g., phase contrast or fluorescence). The components of this instrument are fully integrated and easy to set up. In a BioStation IM, cells are easily maintained at a constant temperature (37 °C) and relative humidity (85 %) in a 5 % CO<sub>2</sub> atmosphere. The BioStation IM enables time-lapse data to be collected reliably over hours or days without focus or image drift. In time-lapse experiments, images can be collected as quickly as 12 frames/s. In a BioStation IM, imaging can be also performed in the X-, Y-, and Z-direction. The unit comes with a well-designed software package and a GUI for controlling the instrument and all experimental parameters.

The BioStation IM is available in two models, the BioStation II and BioStation II-P, optimized for either glass bottom or plastic bottom culture dishes, respectively, and the magnification range is different in the two models. Both models accommodate 35 and 60 mm culture dishes. A four-chambered culture dish, the Hi-Q4 sold by Nikon, can be used for examining four different conditions of culture in the same experiment.

## 8.3 Software Used for Video Bioinformatics Analysis of Stem Cell Morphology and Dynamics

### 8.3.1 CL-Quant

CL-Quant (DRVision, Seattle, WA) provides tools for developing protocols for recognition and quantitative analysis of images and video data [1]. The software is easy to learn and does not require an extensive knowledge of image processing. CL-Quant can be used to detect, segment, measure, analyze, and discover cellular behaviors in video data. It can be used with both phase contrast and fluorescent images. Several basic protocols for cell counting, cell proliferation, wound healing, and cell migration have been created by DRVision engineers and can be obtained when purchasing CL-Quant software. Protocols can be created by DRVision at a user's request, or users can create their own protocols. Later in this chapter, we will describe how to create a protocol in CL-Quant, show the difference between a professional protocol and user-generated protocol, and also show an example in which CL-Quant was used to measure hESC spreading in experimental time-lapse videos.



### 8.3.2 ImageJ

ImageJ is a public domain Java-based image-processing program, which was developed at the National Institutes of Health. ImageJ was designed with an open architecture that provides extensibility via plug-ins and recordable macros. A number of tutorials are available on YouTube and are helpful for beginners learning to use this software. ImageJ is compatible with major operating systems (Linux, Mac OS X, and Windows), works with 8-bit color and grayscale, 16-bit integer, and 32-bit floating point images. It is able to read many image formats, and it supports **time**- or z-stacks. There are numerous plug-ins that can be added to ImageJ to help solve many imaging processing and analysis problems. ImageJ is able to perform numerous standard image-processing operations that may be useful in labs dealing with image analysis and video bioinformatics. For example, researchers have used ImageJ to quantify bands in western blots and also to quantify the fluorescent intensity on the images. One of the advantages of using ImageJ is that it enables rapid conversion of images to different formats. For example, ImageJ can convert tif images to avi, it can create 3D images from z-stacks with 360° rotation, and it can be used to obtain ground truth information when setting up a new video bioinformatics protocol.

## 8.4 Protocols for Cell Attachment and Spreading

In toxicological assays using stem cells, endpoints of interest often occur days or sometimes a month after the experiment begins [27, 37]. There has been interest in shortening such assays, often by using molecular biomarkers to obtain endpoints more rapidly [6]. In the mouse embryonic stem cells test, endpoints can now be obtained in 7 days using biomarkers for heart development. While this significantly reduces the time to reach an endpoint, it is still a relatively long time to obtain data on cytotoxicity.

Pluripotent hESC model the epiblast stage of development [31] and are accordingly a valuable resource for examining the potential effects of chemicals at an early stage of human prenatal development [38]. We are developing video assays to evaluate cellular processes in hESC in short-term cultures, and we then use these assays to identify chemicals that are cytotoxic to young embryos. One hESC-based assay involves evaluation of cell spreading, a dynamic process dependent on the cytoskeleton. When a treatment alters the cytoskeleton or its associated proteins, cells are not able to attach and spread normally. We have used two video bioinformatics protocols to analyze these parameters during 4 h of in vitro culture. At the beginning of cell plating, hESC are round and unattached. Usually, hESC attach to their substrate and begin spreading within 1 h of plating. As cells attach and start spreading, their area increases, and this can be measured in time-lapse images using video bioinformatics tools, thereby providing a rapid method to evaluate a process

137 dependent on the cytoskeleton. Two parameters can be derived from the time-lapse  
138 data: rate of cell spreading (slope) and fold increase in cell area. These two  
139 parameters were compared in control and treated groups using the linear regression  
140 and 2-way ANOVA analysis (GraphPad Prism, San Diego).

141 We will compare two protocols for measuring cell spreading in this chapter.  
142 Both protocols are performed using CL-Quant software. One, which we term a  
143 professional protocol, was created by DRVision engineers for quantifying cell  
144 proliferation. Even though the professional protocol was not created specifically for  
145 hESC spreading, we were able to use the segmentation portion of the protocol for  
146 measuring spreading (area) of hESC during attachment to Matrigel. In addition, we  
147 created our own protocol using CL-Quant for analyzing the area of hESC colonies  
148 during attachment and spreading. Our method, which we refer to as the  
149 user-generated protocol, was created by an undergraduate student with a basic  
150 background in biology and 1 month of experience with CL-Quant software.

151 hESC were cultured using methods described in detail previously [29]. To create  
152 time-lapse videos for this project, small colonies of hESC were incubated in mTeSR  
153 medium at 37 °C and 5 % CO<sub>2</sub> in a BioStation IM for 4 h. Frames were captured  
154 every minute from 4–5 different fields. When applying either the professional or  
155 user-generated protocol, the first step was to segment the image so as to select  
156 mainly hESC. During segmentation, we used the DRVision's soft matching pro-  
157 cedure, which allowed us to identify the objects of interest. The second step was to  
158 remove noise and small particles/debris that were masked during segmentation. In  
159 the third step, the area of all cells in a field was measured in pixels. The protocol  
160 was applied to all images in time-lapse videos to obtain the area occupied by hESC  
161 when plated on Matrigel and incubated for 4 h. Because the survival efficiency is  
162 low for single cells [43], hESC were plated as small colonies, which normally  
163 attach, spread, and survive well. Figure 8.1a shows phase contrast images of several  
164 small hESC colonies plated on Matrigel at different times over 4 h. In the first  
165 frame, the cells were unattached, as indicated by the bright halo around the  
166 periphery of some cells. During 4 h of incubation, the cells attached to the Matrigel  
167 and spread out. By the last frame, all cells in the field have started to spread.  
168 Figure 8.1a also shows the same images after segmentation, enhancement, and  
169 masking using the professional protocol supplied by DRVision. Comparison of the  
170 phase contrast and segmented sequences shows that the masks fit each cell well.

171 To determine if the measurement data obtained from the professional CL-Quant  
172 protocol were accurate, ground truth was obtained by tracing each hESC in all of  
173 the video images using the freehand selection tool in ImageJ, and then measuring  
174 the pixel area for each frame. The ground truth (dotted line) and CL-Quant derived  
175 area were very similar for hESC grown in control conditions (mTeSR medium)  
176 (Fig. 8.1b). For most videos, CL-Quant slightly overestimated the area of the cells  
177 due to difficulty in fitting a perfect mask to each cell.



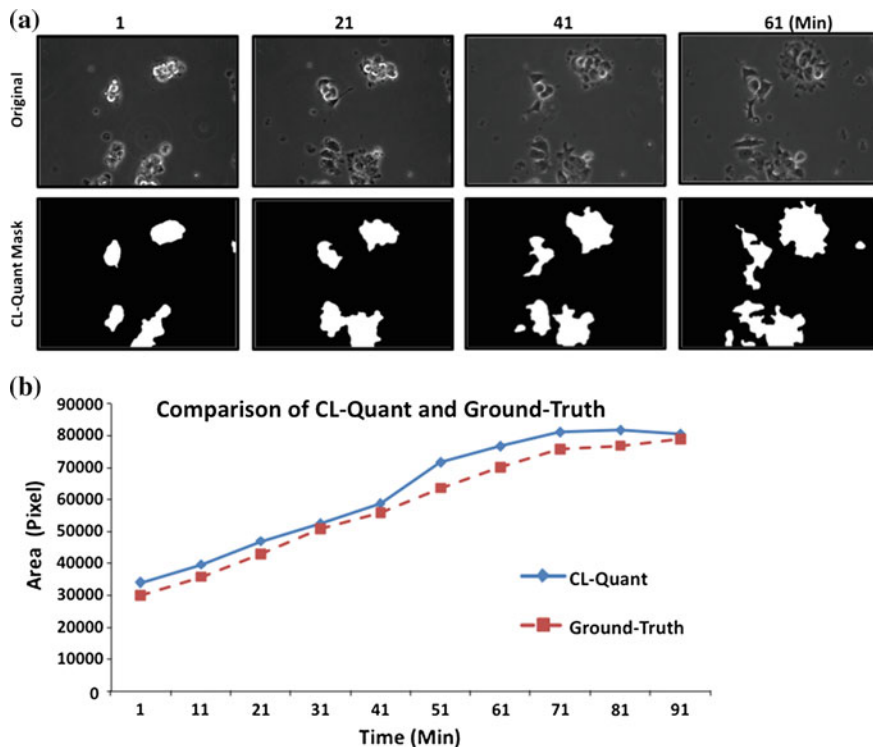


**Fig. 8.1** Comparison of CL-Quant segmentation protocol and ground truth. hESC were plated in mTeSR medium in a 35 mm dish and incubated in a BioStation IM for 4 h. **a** Phase contrast images modified with ImageJ to remove text labels and the same images with masks applied using the professional CL-Quant protocol. **b** Graph showing cell area (spreading) in pixels for CL-Quant derived data and the ground truth. The areas obtained from the two methods were in good agreement

## 8.5 Application of Video Bioinformatics Protocols to hESC Cell Spreading in the Presence of Rock Inhibitors and Blebbistatin

In 2007, ROCK inhibitor (Y27632) was shown to increase the efficiency of hESC survival in culture [43]. However, ROCK is involved in numerous signaling pathways, and therefore may affect many cell properties [25]. ROCK inhibitors decrease non-muscle myosin II activity, and this decrease helps attachment of hESC. However, when single hESC are plated with ROCK inhibitor, they do not adhere to each other due to downregulation of e-cadherin [19]. In addition, hESC treated with Y27632, a potent ROCK inhibitor, appeared stressed and less healthy than untreated controls [3]. Finally, the use of ROCK inhibitor (Y27632) in a toxicological study with methyl mercury decreased the  $IC_{50}$  [11]. Blebbistatin, an

inhibitor of myosin II which is downstream of ROCK, can also be used to increase attachment of hESC and thereby improve plating efficiency [19] and may also alter cell morphology [21].

In this study, time-lapse data were collected on hESC treated with different ROCK inhibitors or blebbistatin, and two CL-Quant protocols were used to quantitatively compare spreading of treated cells to controls. H9 hESC were seeded on Hi-Q4 dishes coated with Matrigel and incubated using different treatment conditions. Cells were then placed in a BioStation IM and cultured as described above for 4 h during which time images were taken at three or four different fields in each treatment/control group at 1 min intervals.

The protocols described in Sect. 1.4 for quantifying hESC area were used to compare spreading of cells subjected to different ROCK inhibitors (Y27632, H1152) or to blebbistatin. First, the written data that was stamped on each image by the BioStation software was removed using the remove outlier's feature in ImageJ. The professional CL-Quant protocol was applied to the resulting time-lapse videos. Examples of phase contrast and masked images are shown in Fig. 8.2 for treatment with the two ROCK inhibitors and blebbistatin. Cells in each group were masked accurately by the segmentation protocol, and even thin surface cell projections were masked with reasonable accuracy. The measurement protocol was then applied to each frame to determine the area (pixels) of the masked cells. To establish the accuracy of this protocol, the ground truth for control and treated groups was determined using ImageJ in two separate experiments (Fig. 8.3a, b). Each point in Fig. 8.3 is the mean of 3 or 4 videos. As shown in Fig. 8.3, the ground truth and the CL-Quant derived data were in good agreement for all groups in both experiments.

In the first experiment, the fold increase in spread area was elevated by Y27632 and blebbistatin relative to the control ( $p < 0.0001$  for Y27632 and  $p < 0.05$  for blebbistatin 2-way ANOVA, Graphpad Prism), while H1152 was not significantly different than the control ( $p > 0.05$ ). The rate of spreading, as determined by the slope for each group, was greater in the three treated groups than in the control; however, only the slope for Y27632 was significantly different than the control ( $p < 0.0001$ ) (slopes = 0.124 control; 0.135 H1152; 0.142 blebbistatin; 0.245 Y27632). In this experiment, the Y27632 group was distinct from all other groups in both its rate of spreading and fold increase in spread area. The morphology of the control cells was normal; cells had smooth surfaces with relatively few projections. In contrast, all treated cells had irregular shapes and more projections than the controls (Fig. 8.3a).

In the second experiment, the three treated groups spread faster and more extensively than the control group. All three treated groups were significantly different than the control with respect to fold change in spread area (by 2-way ANOVA  $p < 0.05$  for Y27632 and H1152;  $p < 0.0001$  for blebbistatin). In contrast to the first experiment, the Y27632 group was similar to the other two treatments (Fig. 8.3d). The rate of spreading was greater in the three treated groups than in the control (slope = 0.084 control; 0.117 H1152; 0.150 blebbistatin; 0.136 Y27632), and both Y27632 ( $p < 0.01$ ) and blebbistatin ( $p < 0.001$ ) were significantly different than the control. As seen in the first experiment, all treated cells were

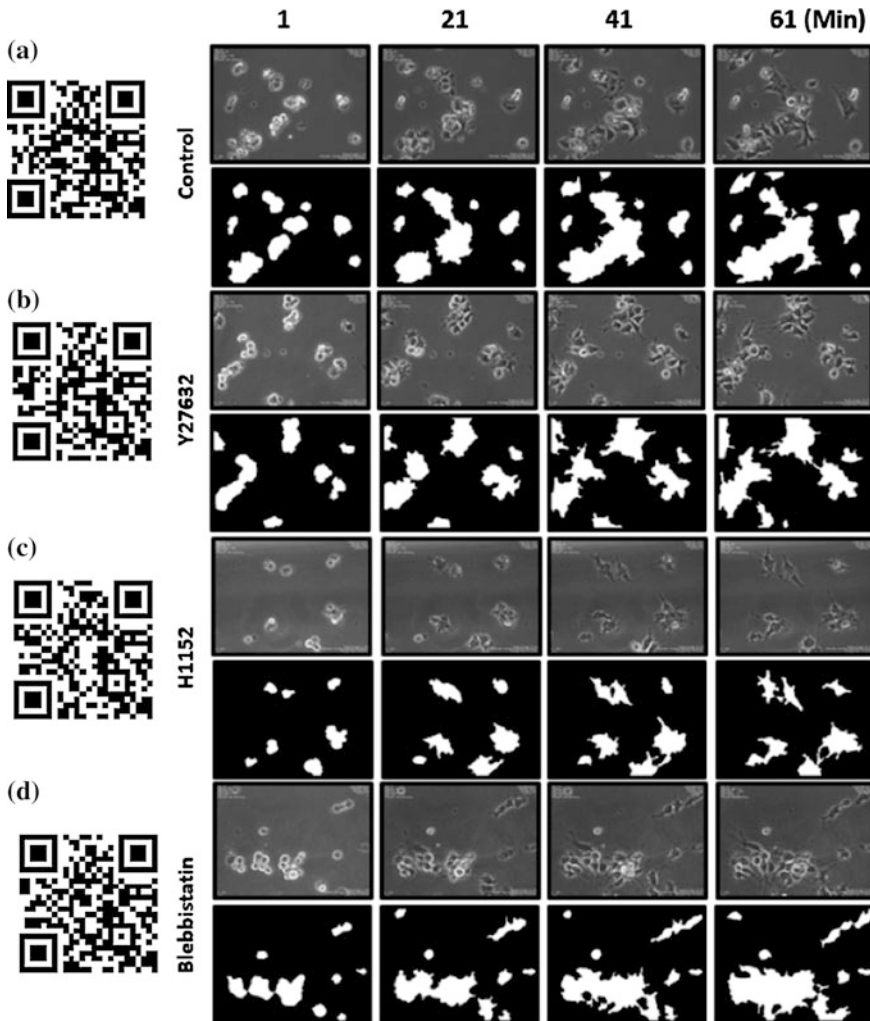


**Fig. 8.2** Cell area (spreading) was successfully masked by the professional CL-Quant protocol in different experimental conditions. hESC were treated with ROCK inhibitors (Y27632 and H1152) or blebbistatin, incubated in a BioStation IM for 4 h, and imaged at 1 min intervals. Phase contrast images and the corresponding masked images are shown for hESC treated with: **a** control medium, **b** Y27632, **c** H1152, and **d** blebbistatin

235 morphologically distinct from the controls. Treated cells appeared attenuated and  
 236 had long thin projections extending from their surfaces, while control cells were  
 237 compact and had smooth surfaces (Fig. 8.3c). It is possible that CL-Quant under-  
 238 estimated the area of the Y27632 inhibitor treated cells in the second experiment  
 239 due to the attenuation of the surface projections, which were more extensive than in  
 240 the first experiment and were difficult to mask accurately.

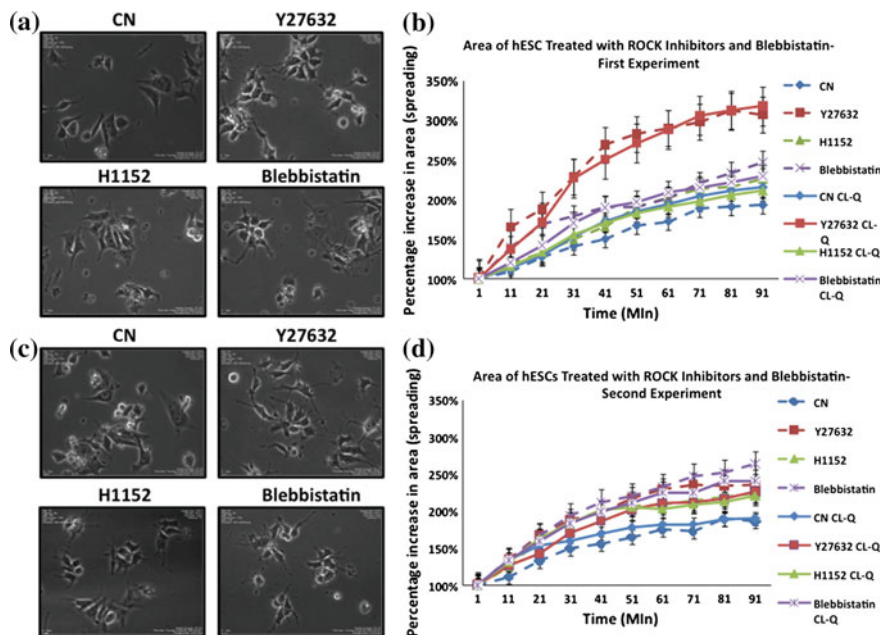


**Fig. 8.3** The morphology and spreading of hESC was affected by treatment with ROCK inhibitors (Y27632 and H1152) and blebbistatin in two experiments. Spreading was measured using the professional CL-Quant protocol. **a** Phase contrast images from the first experiment showed that treated cells were morphologically different than the control. **b** The rate of spreading and the fold increase in spread area was greater in Y27632 and blebbistatin treated cells than in controls. **c** Phase contrast images of control and treated cells in the second experiment showed morphological changes in the treated groups. **d** The fold increase in spread area was greater in the treated cells than in the controls in the second experiment; however, the effect of Y27632 was not as great as previously seen. Data in **(b)** and **(d)** are plotted as a percentage of the area in the first frame. Each point is the mean  $\pm$  the SEM

241 Videos showing the effect of ROCK inhibitors and blebbistatin on hESC  
 242 spreading can be viewed by scanning the bar code.

## 243 8.6 Comparison of Professional and User-Generated 244 Protocols

245 We also compared the professional and user-generated protocols to each other. The  
 246 cells in both the control and treated groups were well masked by the professional  
 247 protocol, and the mask included the thin surface projections characteristic of the  
 248 treated group (Fig. 8.4a). To validate the quantitative data obtained with the pro-  
 249 fessional protocol, ground truth was determined using ImageJ (Fig. 8.4b). Both the

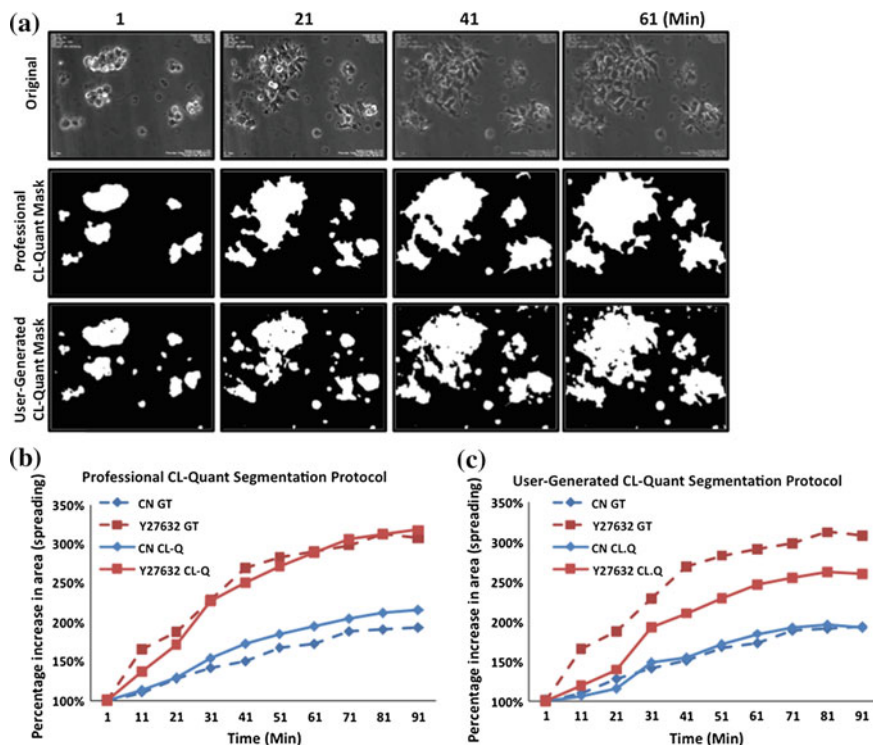


**Fig. 8.4** Comparison of the professional and user-generated cell spreading protocols. **a** Phase contrast micrographs of hESC treated with Y27632 and the corresponding masks created with the professional and user-generated protocols. **b** Comparison of ground truth to area (spreading) data obtained with the professional protocol in control and treated groups. **c** Comparison of ground truth to area (spreading) data obtained with the user-generated protocol in control and treated groups

250 control and treated groups were in good agreement with the ground truth  
 251 (Fig. 8.4b).

252 An advantage CL-Quant is that users can generate their own protocols without a  
 253 programming background. Our user-generated protocol, which was created by an  
 254 undergraduate student with 1 month of experience using CL-Quant, was applied to  
 255 the control and treated groups. The resulting masks did not cover the surface  
 256 projections of the treated group as well as the professional protocol; however, the  
 257 user-generated protocol did include single cells, some of which were filtered out by  
 258 the professional protocol (Fig. 8.4a). The user-generated protocol did not filter out  
 259 the small debris as well as the professional protocol (Fig. 8.4a). The data obtained  
 260 with the user-generated protocol were close to ground truth for the control group,  
 261 but not for the treated group (Fig. 8.4c). Phase contrast images showed that the cells  
 262 treated with Y27632 had many more attenuated surface projections than the control  
 263 cells (Fig. 8.5a, d). Our user-generated protocol and the professional protocol were

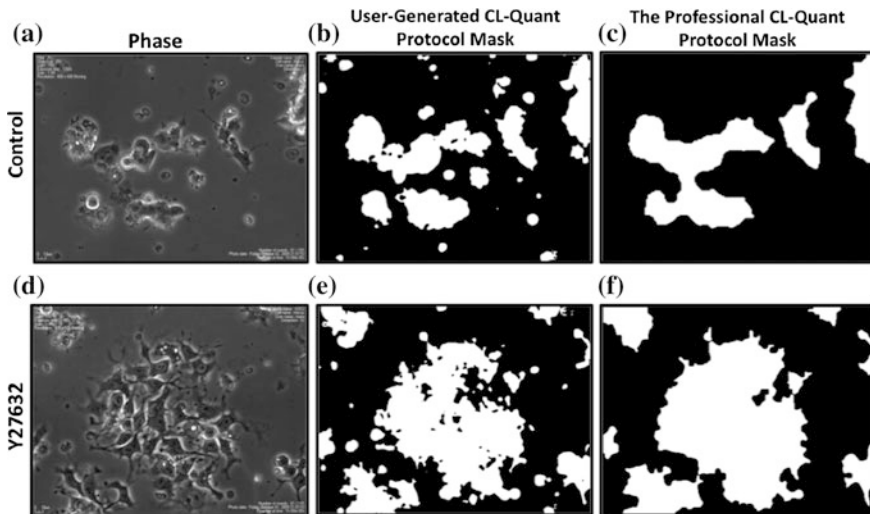


**Fig. 8.5** Differences in cell morphology showing why treated hESC are more difficult to segment than control cells. **a** Phase contrast image of hESC colonies taken at 60 min of incubation. Segmentation of the image in “(a)” created with the user-generated protocol (**b**) and the professional protocol (**c**). **d** Phase contrast image of hESC colonies treated with Y27632 for 60 min. The cells have many thin surface projections not present on controls. Segmentation of the image in “(e)” with the user-generated protocol (**e**) and the professional protocol (**f**)

264 able to mask the control cells well (Fig. 8.5b, c). However, the user-generated  
 265 protocol was not able to mask the thin projections on treated cells as well as the  
 266 professional protocol (Fig. 8.5e, f). Neither protocol recognized gaps between cells  
 267 in the treated group. Overall, the professional protocol was more similar to the  
 268 ground truth than the user-generated protocol in this experiment; however, with  
 269 more experience, the user could improve the protocol to include surface projections  
 270 more accurately.

## 271 8.7 Discussion

272 In this chapter, we introduced a video bioinformatics protocol to quantify cell  
 273 spreading in time-lapse videos using CL-Quant image analysis software, and we  
 274 validated it against ground truth. A professionally developed version of the protocol  
 275 was then compared to a protocol developed by a novice user of CL-Quant. We also  
 276 applied this protocol to hESC treated with blebbistatin and ROCK inhibitors, which  
 277 are commonly used during in vitro passaging of hESC [43].

278 Most evaluations of cells in culture have involved processes such as cell divi-  
 279 sion, confluency and motility, but not spreading. Cell attachment and spreading  
 280 depend on the interaction between cells and the extracellular matrix to which they



281 attach. When cells are plated on a substrate, they first attach, then flatten and spread.  
282 At the molecular level, spreading depends on the interaction of membrane-based  
283 integrins with their extracellular matrix and the engagement of the cytoskeleton,  
284 which initiates a complex cascade of signaling events [7]. This in turn leads to the  
285 morphological changes observed during spreading and enables cultured cells to  
286 flatten out and migrate to form colonies [24, 44].

287 Changes in cell behavior that depend on the cytoskeleton often indicate that cell  
288 health is being compromised by environmental conditions [2, 27]. Because  
289 spreading depends on the cytoskeleton, it can be used to evaluate the effect of  
290 chemical treatments on cytoskeletal health. Cell spreading is a particularly attractive  
291 endpoint in toxicological studies as it occurs soon after plating and does not require  
292 days or weeks of treatment to observe. Many types of cells, such as fibroblasts can  
293 attach and spread in 10–15 min. hESC require about 1–2 h to spread, and therefore  
294 can be plated and data collected in 4 h or less time depending on the experimental  
295 design.

296 The application of the spreading protocol to hESC enables chemical treatments  
297 to be studied using cells that model a very early stage of postimplantation devel-  
298 opment. hESC are derived by isolating and culturing the inner cell mass from  
299 human blastocysts. As these cells adapt to culture, they take on the characteristics of  
300 epiblast cells which are found in young post-implantation embryos [31]. Embryonic  
301 cells are often more sensitive to environmental chemicals than differentiated adult  
302 cells, and it has been argued that risk assessment of environmental chemicals should  
303 be based on their effects on embryonic cells, as these represent the most vulnerable  
304 stage of the life cycle [13]. The sensitivity of hESC to environmental toxicants may  
305 be due to mitochondrial priming which occurs in hESC and makes them more prone  
306 to apoptosis than their differentiated counterparts [26].

307 A major advantage of the cell spreading assay is that it requires relatively little  
308 time to perform. A complete spreading assay can be done in as little as 4 h, while  
309 other endpoints such as cell division and differentiation require days or weeks to  
310 evaluate. The rapidity of the spreading assay makes it valuable in basic research on  
311 the cytoskeleton or in toxicological studies involving drugs or environmental  
312 chemicals. Moreover, this tool could be used in the future as a quality control check  
313 when evaluating stem cell health for clinical applications.

314 The cell spreading assay introduced in this chapter provides a rapid method for  
315 evaluating the cytoskeleton and assessing the quality of cells. Using bioinformatics  
316 tools to analyze the video data significantly reduces the time for data analysis [14–  
317 17]. If an experiment is done for 4 h with 1 min intervals between frames, 240  
318 frames would be collected for each video by the end of the experiment. Each group  
319 could have 4–10 different videos. Before we used bioinformatics tools to analyze  
320 our data, cell spreading was analyzed by measuring cell area manually. ImageJ was  
321 used to calculate cell area for each frame. The total time for cell spreading analysis  
322 for each video was about 24 h. The CL-Quant bioinformatics protocol, which we  
323 introduced in this chapter, greatly reduces this time. In general, it takes about 30–  
324 60 min to create a protocol for a specific purpose. Once the protocol is created, it  
325 takes 5 min to run the protocol using CL-Quant. The protocol can be batch run on



Author Proof

326 multiple videos without requiring users to tie up valuable time performing analysis  
327 of spreading.

328 Our data show that the professionally developed protocol performed better than  
329 the one developed by the novice user. However, the novice was able to rapidly learn  
330 to use CL-Quant software, and he obtained accurate control data as shown by  
331 comparison to the ground truth. It was clear that the novice had difficulty masking  
332 the fine projections on the hESC surfaces, but with additional training, he would  
333 likely be able to create a better segmentation protocol and achieve more accurate  
334 masking of the treated group data.

335 We also examined the effect of ROCK inhibitors and blebbistatin on hESC  
336 spreading. The ROCK inhibitors and blebbistatin improved cell attachment and  
337 spreading, as reported by others [19, 43]. However, those hESC treated with ROCK  
338 inhibitors or blebbistatin appeared stressed, had thin attenuated projections off their  
339 surfaces, and did not seem as healthy as control cells. ROCK inhibitor or blebb-  
340 istatin are often used to improve cell survival, especially when plating single cells.  
341 ROCK inhibitor and blebbistatin allow cells to be accurately counted and plated.  
342 Cell survival is also improved by the efficient attachment observed when these  
343 ROCK inhibitors and blebbistatin are used. Cells are stressed during nucleofection,  
344 so ROCK inhibitors are often used to improve cell survival when nucleofected cells  
345 are ready to plate. ROCK inhibitors and blebbistatin inhibit ROCK protein and  
346 downregulate myosin II activity which accelerates cell attachment and cell  
347 spreading [43]. Our analysis shows that both ROCK inhibitors and blebbistatin alter  
348 the morphology of spreading cells. Moreover, Y27632 and blebbistatin significantly  
349 increased the rate of spreading and the fold change in spread area when compared to  
350 untreated controls, which may be a factor in why they are more commonly used  
351 than H1152. While the full significance of the above changes in cell morphology  
352 and behavior are not yet known, these inhibitors do either indirectly or directly  
353 decrease myosin II activity, which may lead to the stressed appearance of the  
354 treated cells. It has not yet been established why decreasing myosin II activity leads  
355 to more rapid and extensive spreading of hESC.

356 Use of ROCK inhibitors is not recommended in toxicological applications of  
357 hESC as they can alter  $IC_{50}$ s [11]. A spectrophotometer method has been estab-  
358 lished to determine cell number when hESC are in small colonies [4]. This method  
359 enables an accurate number of cells to be plated without the use of ROCK inhibitors  
360 and may generally be applicable to hESC culture and would avoid the morpho-  
361 logical stress observed in ROCK inhibitor treated cells.

362 The protocols reported in this chapter can be used to quantify two parameters of  
363 cell spreading, rate and fold change. The use of spreading as an assay for cyto-  
364 skeletal responses and cell health is attractive as it takes relatively little time to  
365 collect data and analyze data with the application of video bioinformatics tools. In the  
366 future, the segmentation and filtering aspects of these protocols may be improved to  
367 gather more accurate data on the challenging cell surface projections, but these  
368 protocols in their current form can be reliably applied to spreading of hESC col-  
369 onies. In the future, improvements in software could include more advanced



preprocessing tools, tools for analyzing 3-dimensional data, and tools for analyzing different cell morphologies.

**Acknowledgments** We thank DRVision, Sam Alworth, Ned Jastromb, Randy Myers, and Mike Allegro of Nikon Inc. for their invaluable help with the BioStation IM and CL-Quant software training. Work in this chapter was supported by an NSF IGERT grant on Video Bioinformatics (#DGE 093667), the California Institute for Regenerative Medicine (CIRM NE-A0005A-1E), and a grant from the Tobacco-Related Disease Research Program of California (TRDRP 22RT-0127).

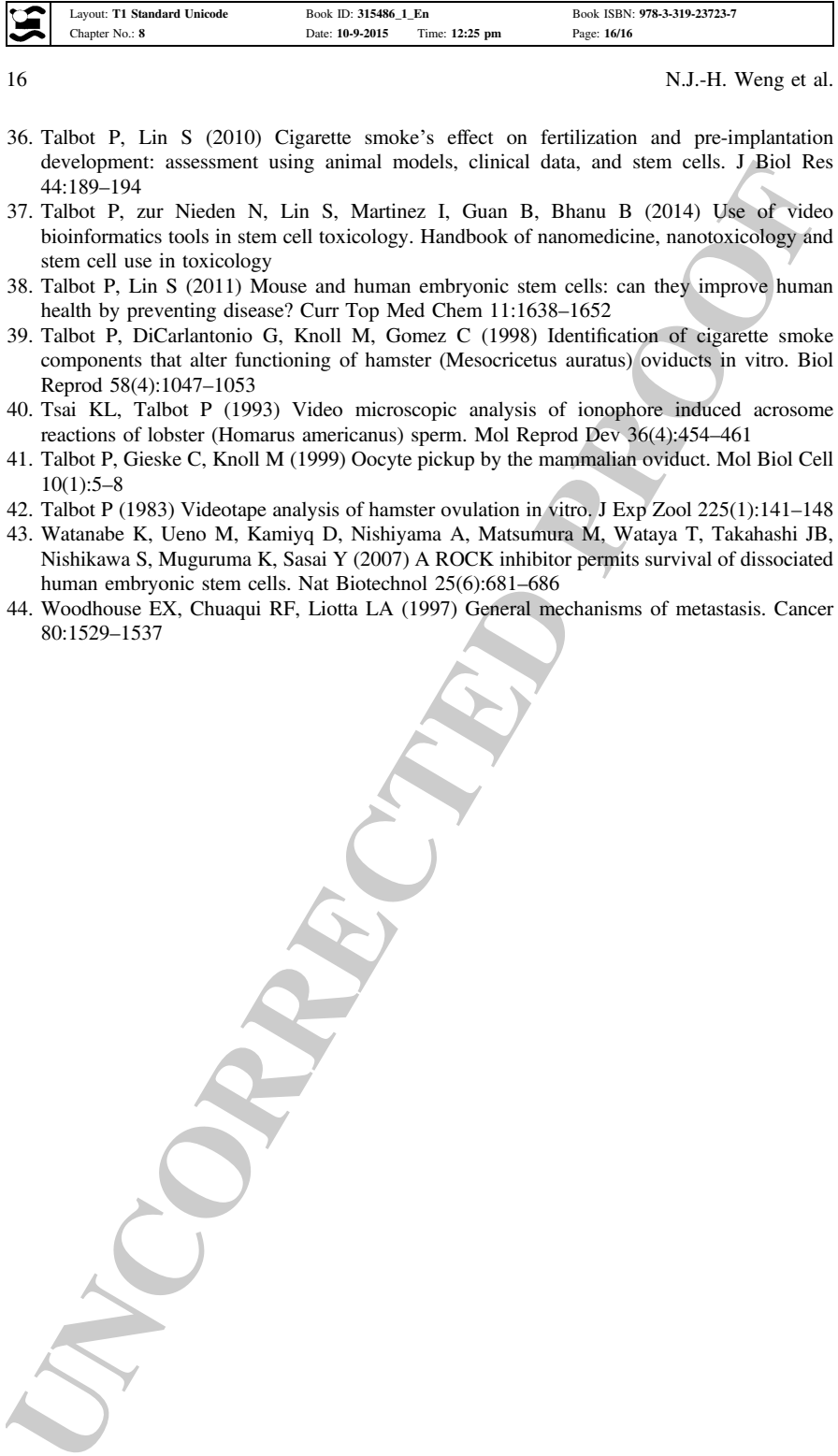
## References

1. Alworth SV, Watanabe H, Lee JS (2010) Teachable, high-content analytics for live-cell, phase contrast movies. *J Biomol Screen* 15(8):968–977. doi:[10.1177/1087057110373546](https://doi.org/10.1177/1087057110373546). 1087057110373546 [pii]
2. Bahl V, Lin S, Xu N, Davis B, Wang Y, Talbot P (2012) Comparison of electronic cigarette refill fluid cytotoxicity using embryonic and adult models. *Reprod Toxicol* 34(4):529–537. doi:[10.1016/j.reprotox.2012.08.001](https://doi.org/10.1016/j.reprotox.2012.08.001)
3. Behar RZ, Bahl V, Wang Y, Weng J, Lin SC, Talbot P (2012) Adaptation of stem cells to 96-well plate assays: use of human embryonic and mouse neural stem cells in the MTT assay. *Curr Protocols Stem Cell Biol Chapter 1(Unit1C):13*
4. Behar RZ, Bahl V, Wang Y, Lin S, Xu N, Davis B, Talbot P (2012) A method for rapid dose-response screening of environmental chemicals using human embryonic stem cells. *J Pharmacol Toxicol Methods* 66:238–245. doi:[10.1016/j.vascn.2012.07.003](https://doi.org/10.1016/j.vascn.2012.07.003)
5. Behar RZ, Davis B, Wang Y, Bahl V, Lin S, Talbot P (2014) Identification of toxicants in cinnamon-flavored electronic cigarette refill fluids. *Toxicol In Vitro*. doi:[10.1016/j.tiv.2013.10.006](https://doi.org/10.1016/j.tiv.2013.10.006)
6. Buesen Roland, Genschow Elke, Slawik Birgitta, Visan Anke, Spielmann Horst, Luch Andreas, Seiler Andrea (2009) Embryonic stem cell test remastered: comparison between the validated EST and the new molecular FACS-EST for assessing developmental toxicity in vitro. *Toxicol Sci* 108(2):389–400
7. Cuvelier D, Theyry M, Chu YS, Thiery JP, Bornens M, Nassory P, Mahadevan L (2007) The universal dynamics of cell spreading. *Curr Biol* 17(8): 694–699
8. Cervinka M, Cervinkova Z, Rudolf E (2008) The role of time-lapse fluorescent microscopy in the characterization of toxic effects in cell populations cultivated in vitro. *Toxicol In Vitro* 22(5):1382–1386. doi:[10.1016/j.tiv.2008.03.011](https://doi.org/10.1016/j.tiv.2008.03.011). S0887-2333(08)00082-9 [pii]
9. DiCarlantonio G, Shaoulian R, Knoll M, Magerts T, Talbot P (1995) Analysis of ciliary beat frequencies in hamster oviducal explants. *J Exp Zool* 272(2):142–152
10. DiCarlantonio G, Talbot P (1999) Inhalation of mainstream and sidestream cigarette smoke retards embryo transport and slows muscle contraction in oviducts of hamsters (*Mesocricetus auratus*). *Biol Reprod* 61(3):651–656
11. Fujimura M, Usuki F, Kawamura M, Izumo S (2011) Inhibition of the Rho/ROCK pathway prevents neuronal degeneration in vitro and in vivo following methylmercury exposure. *Toxicol Appl Pharmacol* 250(1):1–9
12. Gieseke C, Talbot P (2005) Cigarette smoke inhibits hamster oocyte pickup by increasing adhesion between the oocyte cumulus complex and oviductal cilia. *Biol Reprod* 73(3): 443–451
13. Grandjean P, Bellinger D, Bergman A, Cordier S et al (2007) The Faroes statement: human health effects of developmental exposure to chemicals in our environment. *Basic Clin Pharmacol* 102:73–75



- 416 14. Guan BX, Bhanu B, Thakoor N, Talbot P, Lin S (2011) Human embryonic stem cell detection  
417 by spatial information and mixture of Gaussians. In: IEEE first international conference on  
418 healthcare informatics, imaging and systems biology, pp 307–314
- 419 15. Guan BX, Bhanu B, Talbot P, Lin S (2012) Detection of non-dynamic blebbing single  
420 unattached human embryonic stem cells. IEEE Int Conf Image Process 2293–2296
- 421 16. Guan BX, Bhanu B, Talbot P, Lin S (2012) Automated human embryonic stem cell detection.  
422 In: IEEE second international conference on healthcare informatics, imaging and systems  
423 biology (HISB). doi:[10.1109/HISB.2012.25](https://doi.org/10.1109/HISB.2012.25)
- 424 17. Guan BX, Bhanu B, Thakoor N, Talbot P, Lin S (2013) Automatic cell region detection by  
425 K-means with weighted entropy. In: International symposium on biomedical imaging: from  
426 nano to macro, San Francisco, CA
- 427 18. Howard DR, Talbot P (1992) In vitro contraction of lobster (*Homarus*) ovarian muscle:  
428 methods for assaying contraction and effects of biogenic amines. J Exp Zool 263(4):356–366
- 429 19. Harb N, Archer TK, Sato N (2008) The Rho-ROCK-Myosin signaling axis determines  
430 cell-cell integrity of self-renewing pluripotent stem cells. PLoS One 3(8):e3001
- 431 20. Huang S, Driessen N, Knoll M, Talbot P (1997) In vitro analysis of oocyte cumulus complex  
432 pick-up rate in the hamster *Mesocricetus auratus*. Molec Reprod Develop 47:312–322
- 433 21. Holm F, Nikdin H, Kjartansdottir K et al (2013) Passaging techniques and ROCK inhibitor  
434 exert reversible effects on morphology and pluripotency marker gene expression of human  
435 embryonic stem cell lines. Stems Cells Dev 22:1883–1892
- 436 22. Knoll M, Talbot P (1998) Cigarette smoke inhibits oocyte cumulus complex pick-up by the  
437 oviduct in vitro independent of ciliary beat frequency. Reprod Toxicol 12(1):57–68
- 438 23. Knoll M, Shaoulian R, Magers T, Talbot P (1995) Ciliary beat frequency of hamster oviducts  
439 is decreased in vitro by exposure to solutions of mainstream and sidestream cigarette smoke.  
440 Biol Reprod 53(1):29–37
- 441 24. Lauffenburger DA, Horwitz AF (1996) Cell migration: a physically integrated molecular  
442 process. Cell 84:359–369. doi:[10.1016/S0092-8674\(00\)81280-5](https://doi.org/10.1016/S0092-8674(00)81280-5)
- 443 25. Liao JK, Seto M, Noma K (2007) Rho Kinase (ROCK) inhibitors. J Cardiovasc Pharmacol 50  
444 (1):17–24
- 445 26. Liu JC, Guan X, Ryan JA, Rivera AG, Mock C, Agarwal V, Letai A, Lerou PH, Lahav G  
446 (2013) High mitochondrial priming sensitizes hESCs to DNA-damage-induced apoptosis. Cell  
447 Stem Cell 13(4):483–491
- 448 27. Lin S, Fonteno S, Weng J-H, Talbot P (2010) Comparison of the toxicity of smoke from  
449 conventional and harm reduction cigarettes using human embryonic stem cells. Toxicol Sci  
450 118:202–212
- 451 28. Lin S, Fonteno S, Satish S, Bhanu B, Talbot P (2010) Video bioinformatics analysis of human  
452 embryonic stem cell colony growth. J Vis Exp. [http://www.jove.com/index/details.stp?id=](http://www.jove.com/index/details.stp?id=1933)  
453 [1933](http://www.jove.com/index/details.stp?id=1933)
- 454 29. Lin S, Talbot P (2010) Methods for culturing mouse and human embryonic stem cells.  
455 Embryonic stem cell therapy for osteodegenerative disease. Humana Press, pp 31–56
- 456 30. Lin SC, Yip H, Phanthong G, Davis B, Talbot P (2014) Evaluation of cell behavior and  
457 health using video bioinformatics tools. In: Bhanu B, Talbot P (eds) Video bioinformatics,  
458 Chapter 9. Springer, New York
- 459 31. Nichols J, Smith A (2009) Naïve and primed pluripotent states. Cell Stem Cell 4(6):487–492.  
460 doi:[10.1016/j.stem.2009.05.015](https://doi.org/10.1016/j.stem.2009.05.015)
- 461 32. Riveles K, Roza R, Arey J, Talbot P (2004) Pyrazine derivatives in cigarette smoke inhibit  
462 hamster oviductal functioning. Reprod Biol Endocrinol 2(1):23
- 463 33. Riveles K, Roza R, Talbot P (2005) Phenols, quinolines, indoles, benzene, and  
464 2-cyclopenten-1-ones are oviductal toxicants in cigarette smoke. Toxicol Sci 86(1):141–151
- 465 34. Riveles K, Iv M, Arey J, Talbot P (2003) Pyridines in cigarette smoke inhibit hamster  
466 oviductal functioning in picomolar doses. Reprod Toxicol 17(2):191–202
- 467 35. Riveles K, Tran V, Roza R, Kwan D, Talbot P (2007) Smoke from traditional commercial,  
468 harm reduction and research brand cigarettes impairs oviductal functioning in hamsters  
469 (*Mesocricetus auratus*) in vitro. Hum Reprod 22(2):346–355

- 470 36. Talbot P, Lin S (2010) Cigarette smoke's effect on fertilization and pre-implantation  
 471 development: assessment using animal models, clinical data, and stem cells. *J Biol Res*  
 472 44:189–194
- 473 37. Talbot P, zur Nieden N, Lin S, Martinez I, Guan B, Bhanu B (2014) Use of video  
 474 bioinformatics tools in stem cell toxicology. *Handbook of nanomedicine, nanotoxicology and*  
 475 *stem cell use in toxicology*
- 476 38. Talbot P, Lin S (2011) Mouse and human embryonic stem cells: can they improve human  
 477 health by preventing disease? *Curr Top Med Chem* 11:1638–1652
- 478 39. Talbot P, DiCarlantonio G, Knoll M, Gomez C (1998) Identification of cigarette smoke  
 479 components that alter functioning of hamster (*Mesocricetus auratus*) oviducts in vitro. *Biol*  
 480 *Reprod* 58(4):1047–1053
- 481 40. Tsai KL, Talbot P (1993) Video microscopic analysis of ionophore induced acrosome  
 482 reactions of lobster (*Homarus americanus*) sperm. *Mol Reprod Dev* 36(4):454–461
- 483 41. Talbot P, Gieske C, Knoll M (1999) Oocyte pickup by the mammalian oviduct. *Mol Biol Cell*  
 484 10(1):5–8
- 485 42. Talbot P (1983) Videotape analysis of hamster ovulation in vitro. *J Exp Zool* 225(1):141–148
- 486 43. Watanabe K, Ueno M, Kamiyq D, Nishiyama A, Matsumura M, Wataya T, Takahashi JB,  
 487 Nishikawa S, Muguruma K, Sasai Y (2007) A ROCK inhibitor permits survival of dissociated  
 488 human embryonic stem cells. *Nat Biotechnol* 25(6):681–686
- 489 44. Woodhouse EX, Chuaqui RF, Liotta LA (1997) General mechanisms of metastasis. *Cancer*  
 490 80:1529–1537



# Author Query Form

Book ID : **315486\_1\_En**

Chapter No.: **8**



**Springer**

the language of science

Please ensure you fill out your response to the queries raised below and return this form along with your corrections

Dear Author

During the process of typesetting your chapter, the following queries have arisen. Please check your typeset proof carefully against the queries listed below and mark the necessary changes either directly on the proof/online grid or in the 'Author's response' area provided below

Query Refs.	Details Required	Author's Response
<a href="#">AQ1</a>	No queries.	

# MARKED PROOF

## Please correct and return this set

Please use the proof correction marks shown below for all alterations and corrections. If you wish to return your proof by fax you should ensure that all amendments are written clearly in dark ink and are made well within the page margins.

<i>Instruction to printer</i>	<i>Textual mark</i>	<i>Marginal mark</i>
Leave unchanged	... under matter to remain	Ⓟ
Insert in text the matter indicated in the margin	∧	New matter followed by ∧ or ∧ <sup>Ⓢ</sup>
Delete	/ through single character, rule or underline or ┌───┐ through all characters to be deleted	Ⓞ or Ⓞ <sup>Ⓢ</sup>
Substitute character or substitute part of one or more word(s)	/ through letter or ┌───┐ through characters	new character / or new characters /
Change to italics	— under matter to be changed	↵
Change to capitals	≡ under matter to be changed	≡
Change to small capitals	≡ under matter to be changed	≡
Change to bold type	~ under matter to be changed	~
Change to bold italic	≈ under matter to be changed	≈
Change to lower case	Encircle matter to be changed	≡
Change italic to upright type	(As above)	⊕
Change bold to non-bold type	(As above)	⊖
Insert 'superior' character	/ through character or ∧ where required	Υ or Υ under character e.g. Υ or Υ
Insert 'inferior' character	(As above)	∧ over character e.g. ∧
Insert full stop	(As above)	⊙
Insert comma	(As above)	,
Insert single quotation marks	(As above)	ʹ or ʸ and/or ʹ or ʸ
Insert double quotation marks	(As above)	“ or ” and/or ” or ”
Insert hyphen	(As above)	⊥
Start new paragraph	┌	┌
No new paragraph	┐	┐
Transpose	┌┐	┌┐
Close up	linking ○ characters	○
Insert or substitute space between characters or words	/ through character or ∧ where required	Υ
Reduce space between characters or words		↑